

Optical Coherence Tomography Angiography (OCTA) Quantification through AngioAnalytics™

A compendium of scientific articles and abstracts



December 15, 2017

Dear Congress Attendees,

As the many scientific meetings and congresses around the world have demonstrated, OCT Angiography (OCTA) continues to develop at a rapid pace. Clinical insights are forthcoming daily about the elements needed to move the adoption and accessibility of OCTA, from the retina specialist into daily clinical practice for the general ophthalmologist.

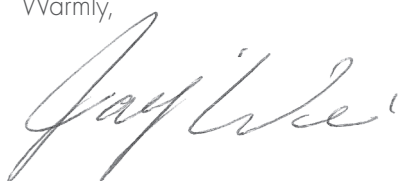
Of paramount importance are improvements in image quality, as it forms the basis not only for accurate qualitative image interpretation, but more significantly, reliable quantitative analysis to enable physicians to easily and quickly document disease states, and hence to incorporate OCTA technology into their diagnostic armamentarium. Quantification tools will shift the treatment paradigm because they provide an objective measure of treatment efficacy, thereby enabling truly customized patient management and improved patient care.

To this end, Optovue has pioneered significant advancements in image quality that will translate into improved quantification. Beyond acquisition of a high-quality image, projection artifact and segmentation errors are two obstacles common to all OCTA technologies, and overcoming them is fundamental to accurate quantitative analysis. The new AngioVue® software, previewed at the 2017 EURETINA Congress and now commercially available, addresses these challenges. Our 3D projection artifact removal (PAR) performs artifact removal pixel-by-pixel throughout the entire 3D volume to remove only artifact, while retaining signal indicative of CNV in the outer retina and choriocapillaris, and in the deep capillary complex. Segmentation errors are addressed first by providing predefined enface slabs and additional retinal layer segmentation so the capillary plexus more closely approximates retinal anatomy, and then by providing proprietary tools to simplify and speed the unavoidable and tedious error correction work.

Optovue's AngioAnalytics™ OCTA quantification technology, first introduced in 2015, leverages these image quality and other improvements to achieve a new level of robustness and relevance that will build diagnostic confidence. Quantitative measurements can enable comparison to normative data for earlier detection of abnormalities, and can be used to track disease progress and treatment efficacy, particularly in slowly progressing diseases such as early diabetic retinopathy. We will continue to advance AngioAnalytics, as we believe quantification is the gateway to widespread and global adoption of OCTA.

Partnerships between the scientific community and industry are the cornerstone to advancing ocular science. I am grateful to our key opinion leaders for their productive relationships with our clinical and medical affairs teams, because this collaborative effort has created innovations that benefit millions of patients across the globe afflicted with sight-threatening diseases. Enjoy your time in Rome at the Fifth International Congress on OCT Angiography, En Face OCT and Advances in OCT!

Warmly,



Jay Wei
Founder and CEO
Optovue, Inc.

Table of Contents

Whitepapers

New AngioVue® Software Streamlines OCTA Interpretation.	3
---	---

Peer-Reviewed Abstracts

Comparison of Quantitative Measurement of Foveal Avascular Zone and Macular Vessel Density in Eyes of Children with Amblyopia and Healthy Controls: An Optical Coherence Tomography Angiography Study. <i>Journal of AAPOS</i> . 2017.	9
Semiautomated Quantitative Approach to Characterize Treatment Response in Neovascular Age-Related Macular Degeneration: A Real-World Study. <i>Retina</i> . 2017.	10
Indocyanine Green Angiography and Optical Coherence Tomography Angiography of Choroidal Neovascularization in Age-Related Macular Degeneration. <i>Invest Ophthalmol Vis Sci</i> . 2017.	11
Optical Coherence Tomography Angiography Reproducibility of Lesion Size Measurements in Neovascular Age-Related Macular Degeneration (AMD). <i>Br J Ophthalmol</i> . 2017.	12
Qualitative and Quantitative Assessment of Vascular Changes in Diabetic Macular Edema after Dexamethasone Implant Using Optical Coherence Tomography Angiography. <i>Int J Mol Sci</i> . 2017.	13
Foveal Avascular Zone Area and Parafoveal Vessel Density Measurements in Different Stages of Diabetic Retinopathy by Optical Coherence Tomography Angiography. <i>Int J Ophthalmol</i> . 2017.	14
Quantifying Microvascular Abnormalities with Increasing Severity of Diabetic Retinopathy Using Optical Coherence Tomography Angiography. <i>Invest Ophthalmol Vis Sci</i> . 2017.	15
Discriminatory Power of Superficial Vessel Density and Prelaminar Vascular Flow Index in Eyes with Glaucoma and Ocular Hypertension and Normal Eyes. <i>Invest Ophthalmol Vis Sci</i> . 2017.	16
Quantitative OCT Angiography of the Retinal Microvasculature and the Choriocapillaris in Myopic Eyes. <i>Invest Ophthalmol Vis Sci</i> . 2017.	17
Retinal Vessel Density in Optical Coherence Tomography Angiography in Optic Atrophy after Nonarteritic Anterior Ischemic Optic Neuropathy. <i>J Ophthalmol</i> . 2017.	18
Quantitative Retinal Optical Coherence Tomography Angiography in Patients with Diabetes without Diabetic Retinopathy. <i>Invest Ophthalmol Vis Sci</i> . 2017.	19
Reduced Retinal Vessel Density in Obstructive Sleep Apnea Syndrome Patients: An Optical Coherence Tomography Angiography Study. <i>Invest Ophthalmol Vis Sci</i> . 2017.	20
Progressive Macula Vessel Density Loss in Primary Open-Angle Glaucoma: A Longitudinal Study. <i>Am J Ophthalmol</i> . 2017.	21
Optical Coherence Tomography Angiography Vessel Density in Children with Type 1 Diabetes. <i>PLoS One</i> . 2017.	22
Optical Coherence Tomography Angiography in Retinal Vein Occlusion: Correlations between Macular Vascular Density, Visual Acuity, and Peripheral Nonperfusion Area on Fluorescein Angiography. <i>Retina</i> . 2017.	23

Bibliography

OCTA Quantification Bibliography: Comprehensive Listing of Peer-Reviewed Articles Highlighting AngioAnalytics™.	24
---	----

New AngioVue® Software Streamlines OCTA Interpretation

Qienyuan Zhou, PhD

Vice President, Clinical Affairs, Optovue, Inc.

Optical coherence tomography angiography (OCTA) with AngioVue® generates depth-resolved images of the vascular structure of the retina and the choroid with capillary details. Previously, interpretation of OCTA data required understanding of projection artifacts throughout the OCTA volume and manually adjusting boundaries of *en face* slabs, which is time-consuming, lacks consistency across observers and makes assessing change over time particularly challenging. The new AngioVue software improves and streamlines OCTA data interpretation by removing projection artifacts from the entire OCTA volume, and by providing predefined *en face* slabs based on appropriately selected anatomical boundaries for consistency across subjects and, within a subject, across visits. This consistency is necessary for both qualitative and quantitative assessment for single visits, and more importantly for assessing change over time.

3D PAR (3D Projection Artifact Removal)

Projection artifacts, common to all OCTA technologies, affect the visualization of the deeper retinal vascular structures, CNV, and choroid. With 3D PAR, projection artifacts are minimized pixel-by-pixel throughout the entire OCTA volume, facilitating clearer visualization of vascular structures in *en face* images and in B-scans at all depths, as illustrated in Fig. 1 (Note the *in-situ* CNV signal more easily visualized in the B-scan with 3D PAR).

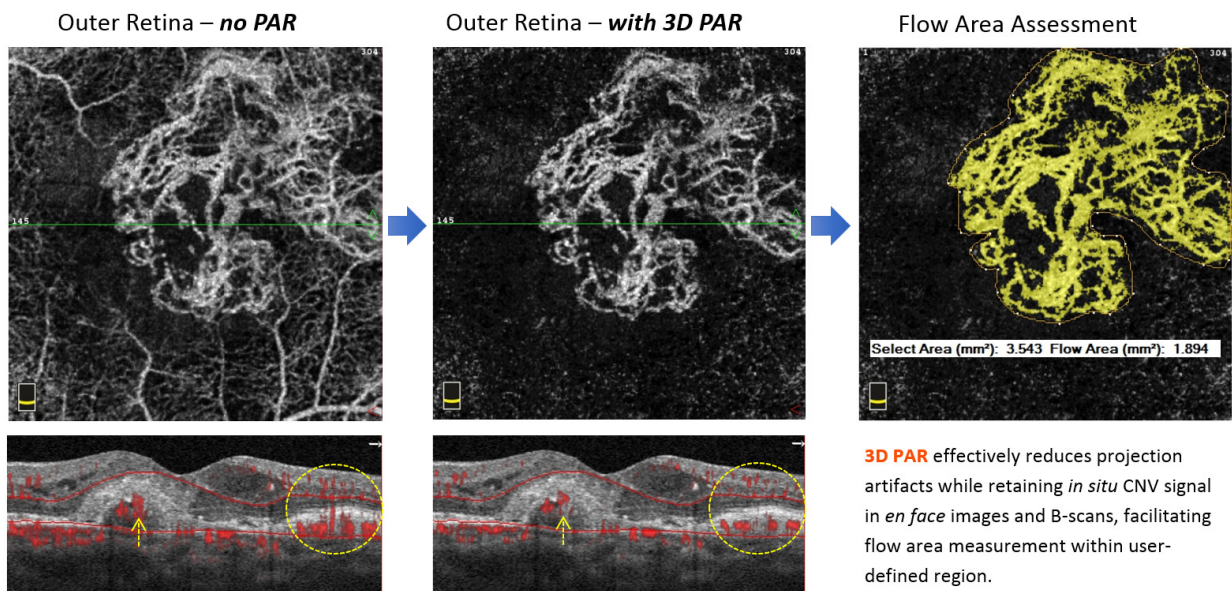
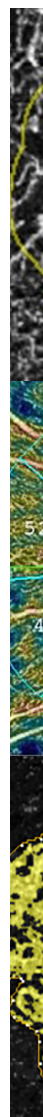


Figure 1: Effectiveness of 3D PAR illustrated in the Outer Retina *en face* image and B-scan image of a CNV case (3mm x 3mm AngioRetina scan). (Image courtesy of Eric D. Nudleman, MD and Michael H. Goldbaum, MD of Shiley Eye Institute, University of California at San Diego, La Jolla, CA.)



New segmentation and predefined *en face* slabs

The new software provides additional retina layer boundaries segmentation, including OPL (outer plexiform layer) outer boundary segmentation and BRM (Bruch’s membrane) boundary segmentation, in addition to previously available segmentation boundaries (ILM, IPL, ISOS, RPE). Predefined *en face* slabs (Fig. 2) are provided within the software, consistent with the slab segmentations recommended by Campbell et al,¹ and enable the following

- The addition of OPL to ILM and IPL facilitates consistent *en face* slab definition across subjects and across visits for the superficial vascular complex (Superficial or SVC, from ILM ~ IPL-10 μ m) slab and deep vascular complex (Deep or DVC, from IPL-10 μ m to OPL+10 μ m) slab.
- The addition of OPL and BRM facilitates the use of predefined *en face* slabs for the outer retina avascular zone (from OPL+10 μ m to BRM-10 μ m), providing a consistent, anatomically appropriate *en face* slab for CNV evaluation across patients and over time.
- The choriocapillaris slab (from BRM-10 μ m to BRM+30 μ m) provides a consistent basis for the evaluation of the choriocapillaris across patients and over time.
- The predefined *en face* slabs provide a consistent basis for vessel density analysis of the Superficial and the Deep vasculature complex (Fig. 3).
- The retinal *en face* slab (Retina, from ILM to OPL+10 μ m) provides a consistent basis for the evaluation of the FAZ (Fig. 3).

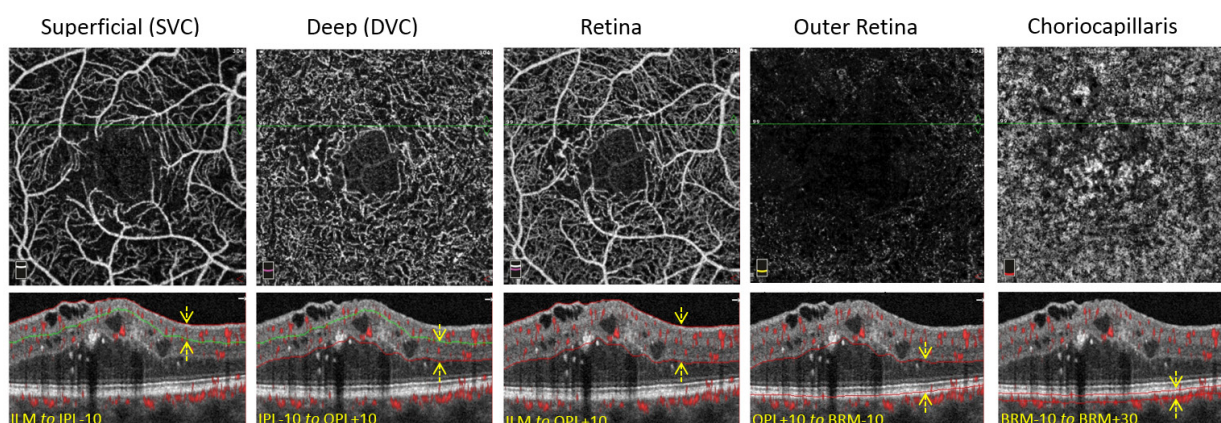


Figure 2: The five predefined *en face* slabs in the software are illustrated with a DR case (3mm x 3mm AngioRetina scan). (Image courtesy of Eric D. Nudleman, MD and Michael H. Goldbaum, MD of Shiley Eye Institute, University of California at San Diego, La Jolla, CA.)

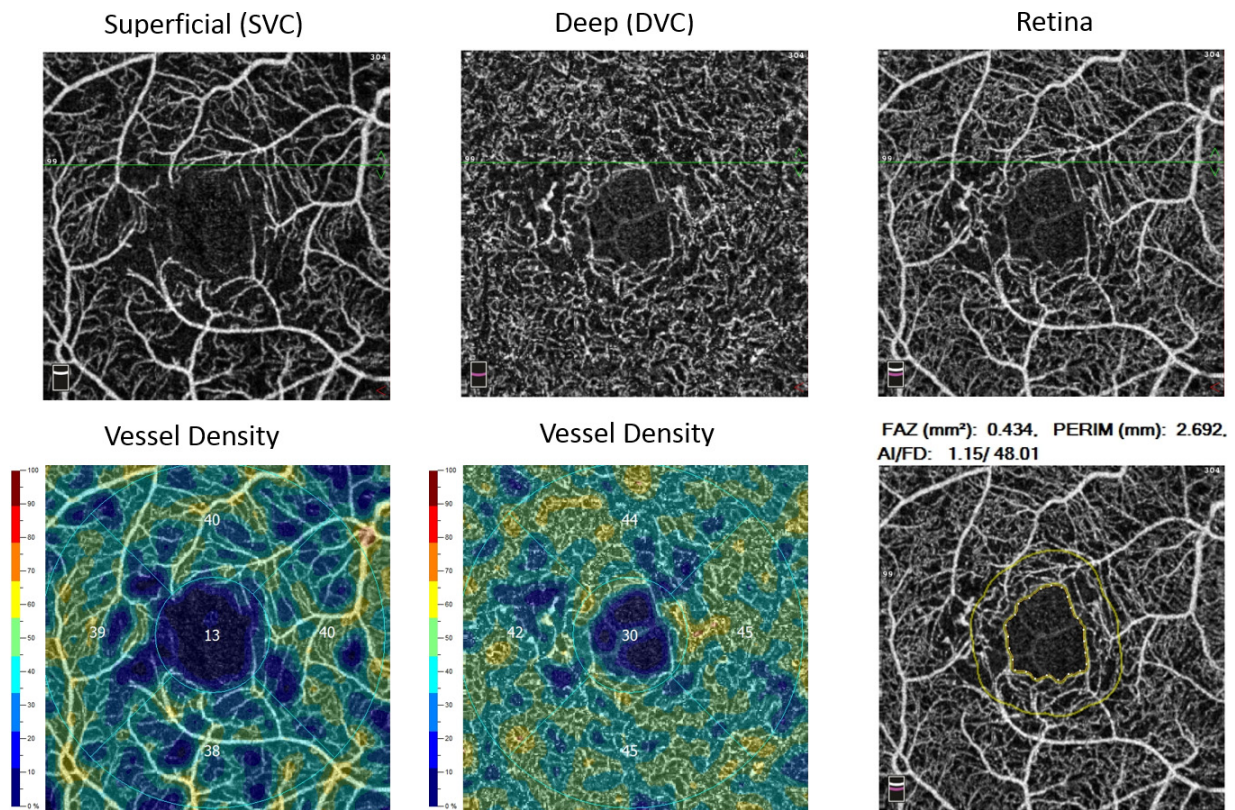
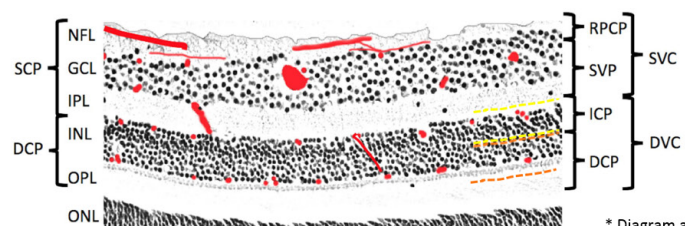


Figure 3: The predefined en face slabs provide consistent basis for vessel density analysis of the Superficial slab and the Deep slab, as well as FAZ analysis of the Retina slab as illustrated with the DR case (3mm x 3mm AngioRetina scan). (Image courtesy of Eric D. Nudleman, MD and Michael H. Goldbaum, MD of Shiley Eye Institute, University of California at San Diego, La Jolla, CA.)

To provide flexibility in *en face* visualization for clinical and research purposes, a custom *en face* slab is provided with user-definable adjustable boundaries. Use of the custom slab in conjunction with 3D PAR facilitates visualization of vasculature in the inner region of the INL (i.e., ICP) and vasculature in the outer region of the INL (i.e., DCP) as illustrated in Fig. 4.

Segmentation editing and automatic propagation

Correct segmentation is required for appropriate and consistent definition of *en face* slabs for qualitative and quantitative evaluation, and for assessing change over time. Error in automatic segmentation can occur in some cases. With the new Edit/Propagation tool, users can manually correct one or a few affected B-scans and propagate the correction throughout the entire scan volume or through a user-selected region in under one second.



* Diagram adapted from Reference 1.

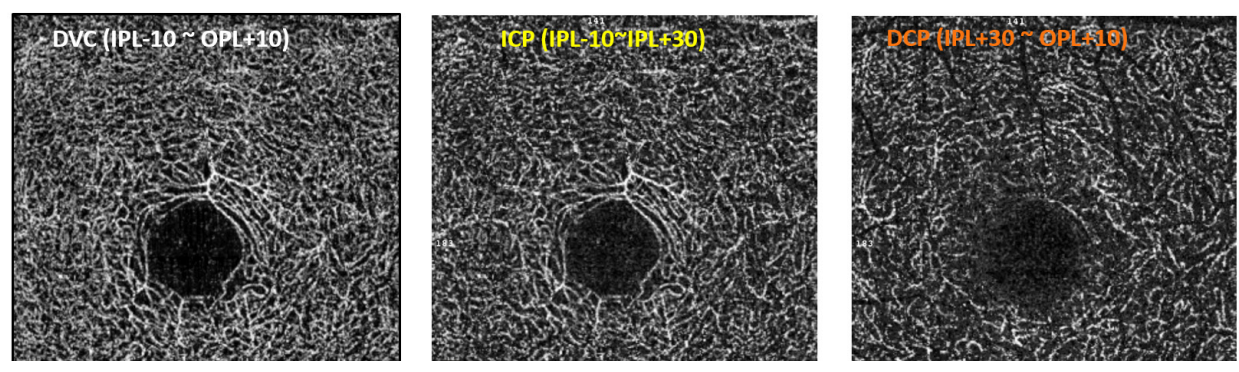


Figure 4: Custom slab can be set to provide en face images of the ICP slab or the DCP slab of a normal case; the predefined DVC slab en face image is shown for comparison (3mm x 3mm AngioRetina scan).

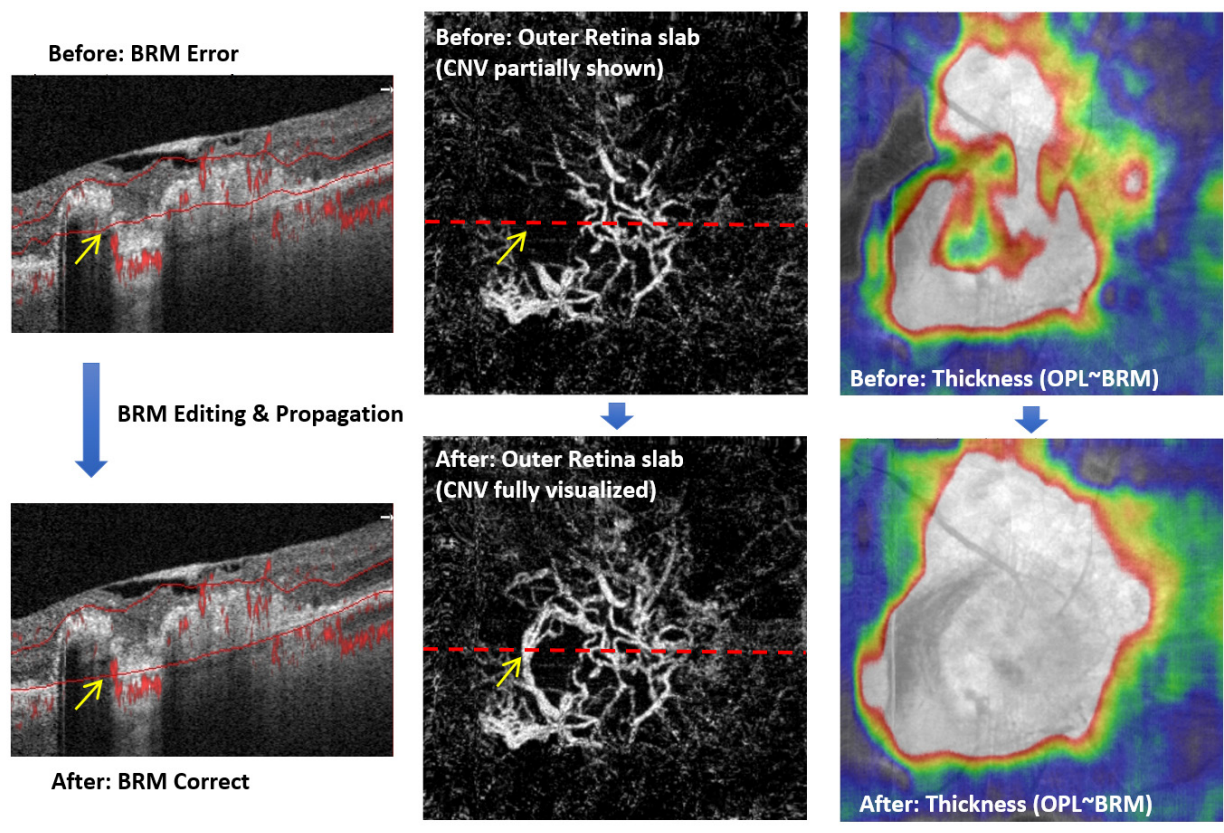


Figure 5: Example of BRM (Bruch's membrane) segmentation editing/propagation in a CNV case (3mm x 3mm AngioRetina scan). (Image courtesy of Pravin Dugel, MD, Retinal Consultants of Arizona, Phoenix, AZ.)

New montage

Large field of view OCTA images, with good capillary details and fast processing time, can be generated through an automatic montage of 2 scans (Fig. 6): one 6mm x 6mm high-density (HD) AngioRetina scan and one 6mm x 6mm HD AngioDisc scan.

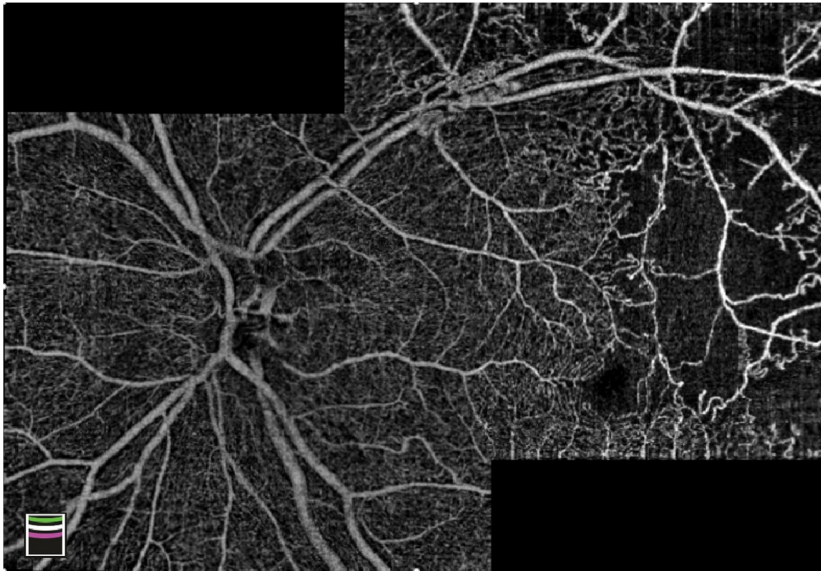


Figure 6: Example of automatic montage of two 6mm x 6mm HD Angio scans of a BRVO case (image courtesy of Theodore Leng, MD, Byers Eye Institute, Stanford University, Palo Alto, CA.)

Assessment of change

The software provides a multi-scan view that effectively facilitates assessment of change over time, benefitting from consistent slab definition and registered B-scans across visits (Fig. 7).

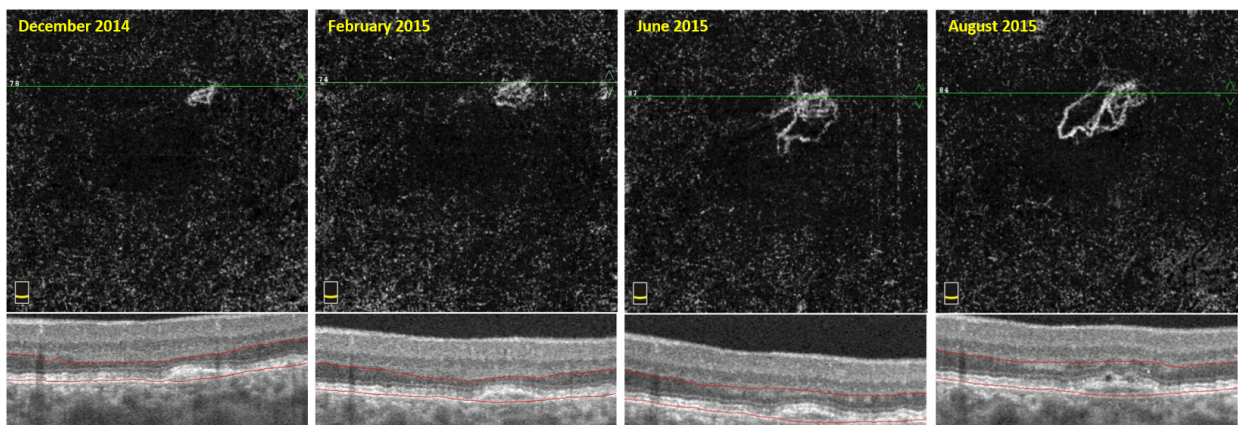


Figure 7: Example of multi-scan view of Outer Retina slab of a CNV case followed longitudinally from December 2014 through August 2015 (3mm x 3mm AngioRetina scans). (Image courtesy of Adil El Maftouhi, OD, Centre Rabelais, Lyon, France.)

New quantitative analysis of RPC vessel density and optic nerve structure

With the simultaneously acquired OCT and OCTA volume of the AngioVue® scan, structural and vascular analyses can be derived in parallel with exact correspondence in analyzed regions. The AngioVue® optic disc scan is particularly advantageous for optic nerve head (ONH) morphological analysis due to minimized distortions from motion artifacts, as a result of previously released DualTrac™ Motion Correction for OCTA imaging. DualTrac comprises two levels of correction for motion artifacts, correction of lateral eye motion artifacts in the 3D volume through active tracking and axial motion artifact correction in the post-processing phase. This is achieved by merging two orthogonally scanned volumes, thus eliminating distortion and preserving the shape of the ONH.

As illustrated in the example below of a 4.5mm x 4.5mm HD AngioDisc scan of a glaucomatous eye (Fig. 8), the new AngioVue software provides ONH analysis, RNFL thickness measurements, and RPC (radial peripapillary capillaries) vessel density analyses. The disc margin is automatically detected based on Bruch's Membrane Opening (BMO), and both cup and rim are measured within the BMO plane. The peripapillary sectors approximate the trajectory of the RNFL bundles, starting with the sector definition initially proposed by Garway-Heath et al,² and adapted to the wider peripapillary region based on work by Tan et al.³

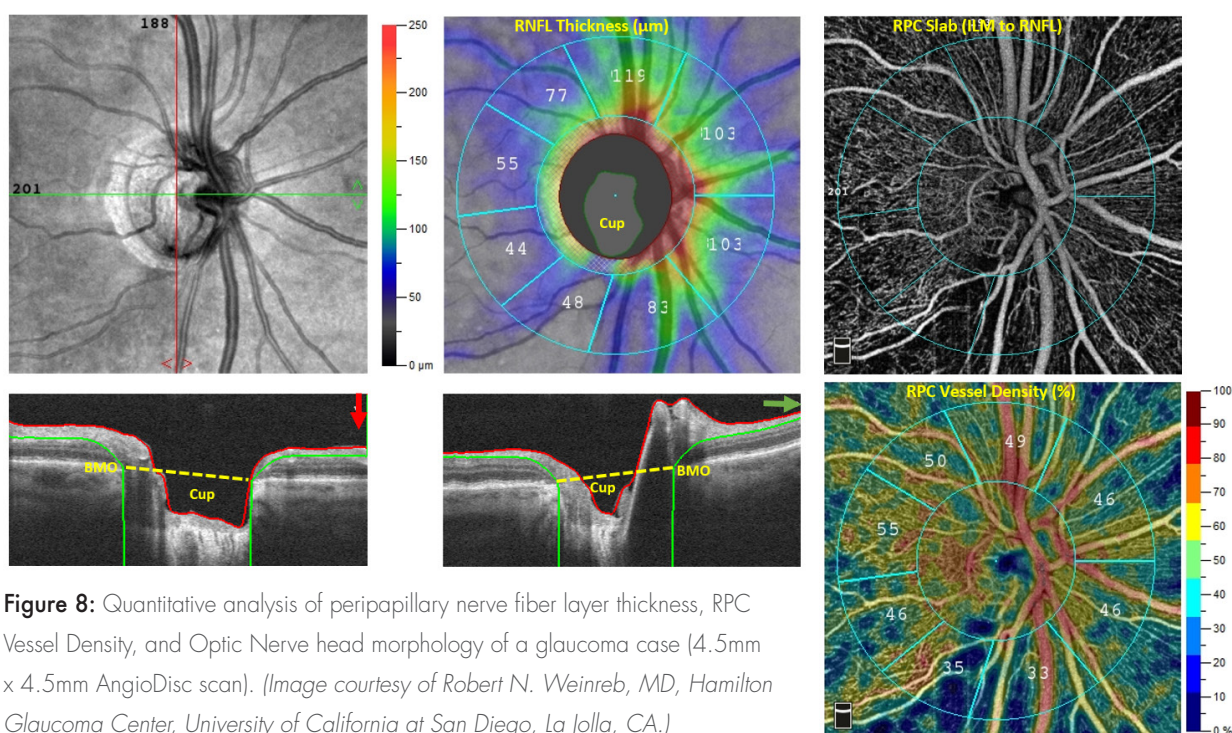


Figure 8: Quantitative analysis of peripapillary nerve fiber layer thickness, RPC Vessel Density, and Optic Nerve head morphology of a glaucoma case (4.5mm x 4.5mm AngioDisc scan). (Image courtesy of Robert N. Weinreb, MD, Hamilton Glaucoma Center, University of California at San Diego, La Jolla, CA.)

The new AngioVue software was developed by the Optovue team of algorithm development scientists, software engineers, clinical scientists and SQA engineers. Note: AngioAnalytics™ software is not FDA-cleared for sale in the U.S.

References:

1. J. P. Campbell*, M. Zhang*, T. S. Hwang, S. T. Bailey, D. J. Wilson, Y. Jia & D. Huang. Detailed Vascular Anatomy of the Human Retina by Projection-Resolved Optical Coherence Tomography Angiography. *Nature Scientific Reports* | 7:42201 (2017) | DOI: 10.1038/srep42201.
2. D. F. Garway-Heath, D. Poinosawmy, F. W. Fitzke, R. A. Hitchings. Mapping the Visual Field to the Optic Disc in Normal Tension Glaucoma Eyes. *Ophthalmology*, 2000 Oct; 107(10): 1809-15.
3. O. Tan, L. Liu, L. Liu, D. Huang. Nerve Fiber Flux Analysis Using Wide-Field Swept Source Optical Coherence Tomography. *Translational Vision Science & Technology*, 2017, in press.



Comparison of Quantitative Measurement of Foveal Avascular Zone and Macular Vessel Density in Eyes of Children with Amblyopia and Healthy Controls: An Optical Coherence Tomography Angiography Study.

Yilmaz I¹, Ocak OB², Yilmaz BS², Inal A², Gokyigit B², Taskapili M².

Purpose

To quantify vessel density of superficial capillary plexus (SCP), deep capillary plexus (DCP), and the foveal avascular zone (FAZ) of children's amblyopic eyes and to compare the measurements with those of companion eyes and age-matched controls.

Methods

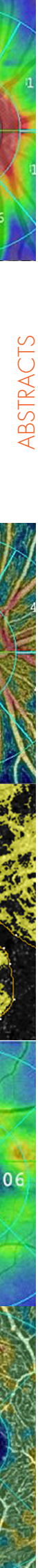
Fifteen patients with strabismic amblyopia, and 15 age-matched controls were included in this cross-sectional study. SCP, DCP, and FAZ were measured via optical coherence tomographic angiography (OCTA).

Results

Mean subject age was 8.2 ± 2.3 years in the amblyopia group and 8.6 ± 2.2 years in the control group. The mean SCP at 1mm, 2mm, and 3mm zones were (in the order amblyopic eye, companion eye, control) 1.399 ± 0.088 , 5.854 ± 0.195 , 12.866 ± 0.346 ; 1.467 ± 0.084 , 5.979 ± 0.182 , 12.965 ± 0.321 ; and 1.559 ± 0.052 , 6.343 ± 0.190 , 13.819 ± 0.423 . SCP was significantly lower in amblyopic eyes than in companion eyes and controls ($P < 0.05$). The mean DCP at 1mm, 2mm, and 3mm zones were 1.425 ± 0.069 , 6.038 ± 0.186 , 13.522 ± 0.336 ; 1.525 ± 0.072 , 6.427 ± 0.190 , 14.286 ± 0.322 ; and 1.685 ± 0.074 , 6.895 ± 0.198 , 15.355 ± 0.356 . DCP was significantly lower in amblyopic eyes than companion eyes and controls ($P < 0.05$). The mean superficial FAZ were 0.287 ± 0.091 , 0.262 ± 0.092 , and 0.280 ± 0.097 . The mean deep FAZ were 0.382 ± 0.092 , 0.335 ± 0.080 , and 0.329 ± 0.085 . There was no significant difference in FAZ among groups ($P > 0.05$).

Conclusions

Vessel density of SCP and DCP of eyes with amblyopia is lower than that of the companion eye and the age-matched controls.



Semiautomated Quantitative Approach to Characterize Treatment Response in Neovascular Age-Related Macular Degeneration: A Real-World Study.

Roberts PK¹, Nesper PL, Gill MK, Fawzi AA.

Purpose

To perform a quantitative study of the vascular microstructure in actively treated choroidal neovascularization by optical coherence tomographic angiography.

Methods

Patients undergoing individualized anti-vascular endothelial growth factor therapy of minimum 12 months duration were included in this cross-sectional observational study and imaged using optical coherence tomographic angiography. En face optical coherence tomographic angiography images were analyzed for quantitative features, such as junction density, vessel length, and lacunarity using validated software (Angiotool). Patients were divided into 2 groups depending on their individualized treatment interval: "good responders, treated less frequently than 6 weeks" versus "poor responders, treated every 6 weeks or more frequently." Nonparametric testing was used to assess differences between these groups.

Results

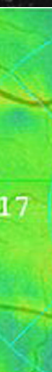
Twenty-five eyes of 23 consecutive patients with a median 58-month history of choroidal neovascularization, treated by median of 34 anti-vascular endothelial growth factor injections, were included in the analysis. There was no significant difference between any of the microvascular choroidal neovascularization features between the 2 groups ($P > 0.05$).

Conclusion

The semiautomated vessel segmentation software provides an objective and quantitative approach for choroidal neovascularization characterization. The consistently nonsignificant outcomes between the groups may provide evidence to support the "normalization hypothesis." This would suggest that regardless of treatment interval, individualized therapy in these eyes established vessel stability.



ABSTRACTS



Indocyanine Green Angiography and Optical Coherence Tomography Angiography of Choroidal Neovascularization in Age-Related Macular Degeneration.

Chiara M. Eandi; Antonio Ciardella; Mariacristina Parravano; Filippo Missiroli; Camilla Alovisi; Chiara Veronese; Maria C. Morara; Massimo Grossi; Gianni Virgili; Federico Ricci.

Purpose

To compare the capability of indocyanine green angiography (ICGA) and optical coherence tomography angiography (OCTA) in detecting choroidal neovascularization (CNV).

Methods

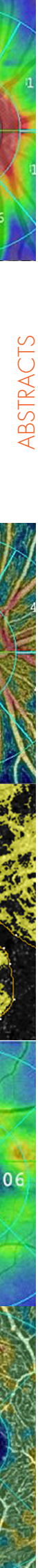
In this prospective study, patients with CNV detected with fluorescein angiography (FA) underwent ICGA and OCTA, spectral domain OCT (SD-OCT), and infrared or fundus color photographs. CNV lesions were outlined on ICGA and OCTA images, and the composition and size of the CNV was documented.

Results

One hundred eighty-two eyes were included. With ICGA, well-defined lesions were observed in 37.9%, partly defined in 44.5%, and undefined in 17% of eyes. On OCTA, well defined, partly defined, and undefined vessels were observed in 53.8%, 27.5%, and 18.7% of eyes, respectively. There was a good correlation between CNV size measured with the two instruments ($r = 0.84$). However, OCTA underestimated CNV area by about 4.5% (slope coefficient with linear regression: 0.55, 95% confidence interval [CI]: 0.46 to 0.65; intercept: 0.27, 95% CI: -0.2 to 0.56). On ICGA, CNV composition was capillary in 28%, mature in 14.3%, and mixed (capillary and major neovascular complex) in 57.7% of eyes. Similarly, OCTA revealed capillary, mature, and mixed CNV in 28.9%, 15.9%, and 55.5% of eyes, respectively.

Conclusions

OCTA provides the clinician the ability to perform precise structural and vascular assessment of CNV noninvasively. Our study is, to our knowledge, the largest OCTA analysis to date of CNV secondary to neovascular AMD analyzed simultaneously by ICGA and OCTA.



Optical Coherence Tomography Angiography Reproducibility of Lesion Size Measurements in Neovascular Age-Related Macular Degeneration (AMD).

Amoroso F^{1,2}, Miere A¹, Semoun O¹, Jung C^{1,3}, Capuano V¹, Souied EH^{1,3}.

Purpose

To evaluate the reproducibility and inter-user agreement of measurements of choroidal neovascularisation in optical coherence tomography angiography (OCTA).

Design

Prospective non-interventional study.

Methods

Consecutive patients, presenting with neovascular age-related macular degeneration (AMD), underwent two sequential OCTA examinations (AngioVue, Optovue, Fremont, CA, USA), performed by the same trained examiner. Neovascular lesion area was then measured on both examinations in the choriocapillaris automatic segmentation by two masked readers, using the semiautomated measuring software embedded in the instrument. Two measuring features were used: the first corresponding to the total manually contoured lesion area with the flow draw tool (select area) and the second to the total area of solely vessels with high flow within the lesion (vessel area). These measurements were then compared in order to assess both the reproducibility of OCTA examination and the interuser agreement with the embedded software.

Results

Forty-eight eyes of 46 patients (77.4 mean age, ± 8.2 SD, range from 62 to 95 years old, eight men, 38 women) were included in our study. Mean choroidal neovascularisation area was of 0.72 ± 0.7 mm² for the first measurement and 0.75 ± 0.7 mm² for the second measurement; difference between the first and the second measurement was 0.03 mm². Intrauser agreement was of 0.98 (CI 0.98 to 0.99) for both 'vessel area' and 'select area' features. Interuser agreement was of 0.98 (CI 0.97 to 0.99) for 'select area' and 'vessel area' features.

Conclusion

Our data suggest that OCTA provide reproducible imaging for evaluation of the neovascular size in the setting of AMD.



Qualitative and Quantitative Assessment of Vascular Changes in Diabetic Macular Edema after Dexamethasone Implant Using Optical Coherence Tomography Angiography.

Lisa Toto¹, Rossella D'Aloisio^{2*}, Marta Di Nicola³, Giuseppe Di Martino⁴, Silvio Di Staso⁵, Marco Ciancaglini,⁵ Daniele Tognetto,² and Leonardo Mastropasqua¹.

Purpose

The aim of this study was to investigate retinal and choriocapillaris vessel changes in diabetic macular edema (DME) after the intravitreal dexamethasone implant (IDI) using optical coherence tomography angiography (OCTA). Moreover, a comparison between morphological and functional parameters of DME and healthy patients was performed.

Methods

Twenty-five eyes of 25 type 2 diabetic retinopathy patients complicated by macular edema (DME group) and 25 healthy subjects (control group) were enrolled. Superficial capillary plexus density (SCPD) and deep capillary plexus density (DCPD) in the foveal and parafoveal areas, choriocapillary density (CCD) and optic disc vessel density (ODVD) were detected using OCTA at baseline and after 7, 30, 60, 90 and 120 days post injection. Best corrected visual acuity (BCVA), retinal sensitivity, and central retinal thickness (CMT) were also evaluated in both groups of patients.

Results

A statistically significant difference between the two groups (DME and controls) was found in terms of functional (MP, $p < 0.001$ and BCVA, $p < 0.001$) and morphological (CMT, $p < 0.001$; SCPD in the parafoveal area, $p < 0.001$; DCPD in the foveal area, $p < 0.05$ and parafoveal area, $p < 0.001$; CCD, $p < 0.001$) parameters. After the treatment, SCPD and DCPD in the foveal and parafoveal areas did not modify significantly during the follow up.

Foveal Avascular Zone Area and Parafoveal Vessel Density Measurements in Different Stages of Diabetic Retinopathy by Optical Coherence Tomography Angiography.

Mastropasqua R¹, Toto L², Mastropasqua A², Aloia R², De Nicola C², Mattei PA², Di Marzio G², Di Nicola M³, Di Antonio L².

Aim

To investigate foveal avascular zone (FAZ) and parafoveal vessel densities (PRVD) by means of optical coherence tomography angiography (OCTA) in diabetic patients with or without diabetic retinopathy (DR) and to assess the reproducibility of FAZ and PRVD measurements.

Methods

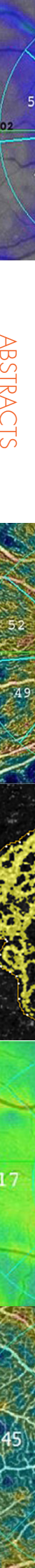
Sixty diabetic patients (60 eyes) with different stage of DR (graded according to the International Clinical Severity Scale for DR) and 20 healthy subjects underwent FAZ area and PRVD measurements using OCTA by two experienced examiners. FAZ area in all patients was also assessed using fluorescein angiography (FA).

Results

In subject with proliferative DR and with moderate-severe non-proliferative DR, FAZ area was significantly increased compared to healthy controls ($P=0.025$ and $P=0.050$ respectively measured with OCTA and $P=0.025$ and $P=0.048$ respectively measured with FA). OCTA showed significantly less inter-observer variability compared to FA. Concordance correlation coefficient (CCC) for FAZ area measurements was 0.829 (95%CI: 0.736–0.891) $P<0.001$ with FA and 1.000 (95%CI: 0.999–1.000) $P<0.001$ with OCTA. CCC was 0.834 (95%CI: 0.746–0.893) $P<0.001$ and 0.890 (95%CI: 0.828–0.930) $P<0.001$ for parafoveal superficial and deep vessel density measurements, respectively.

Conclusion

OCTA shows progressive increase of FAZ area and reduction of PRVD in both superficial and deep plexus at increasing DR severity. FAZ area and PRVD measurements using OCTA are highly reproducible.



Quantifying Microvascular Abnormalities with Increasing Severity of Diabetic Retinopathy Using Optical Coherence Tomography Angiography.

Nesper PL¹, Roberts PK^{1,2}, Onishi AC¹, Chai H^{3,4}, Liu L³, Jampol LM¹, Fawzi AA¹.

Purpose

We quantified retinal and choriocapillaris microvascular changes in healthy control eyes and different stages of diabetic retinopathy (DR) using optical coherence tomography angiography (OCTA).

Methods

This retrospective cross-sectional study included 137 eyes of 86 patients with different stages of DR and 44 eyes of 26 healthy age-matched controls. Participants were imaged with a commercial OCTA device (XR Avanti, AngioVue, Fremont, CA, USA). We analyzed the superficial (SCP) and deep (DCP) retinal capillary plexus, the full retina, and choriocapillaris for the following OCTA parameters: foveal avascular zone, vessel density, percent area of nonperfusion (PAN), and adjusted flow index (AFI). We adjusted for age, sex, and the correlation between eyes of the same study participant in our statistical models.

Results

All OCTA parameters showed a significant linear correlation with DR severity ($P < 0.05$) in the univariate models except for AFI measured in the SCP and these correlations remained significant after correcting for covariates. Compared to the other capillary layers, the AFI at the DCP decreased significantly with DR severity. When comparing individual disease severity groups as categories, eyes of subjects with diabetes without DR had significantly increased PAN and AFI in the SCP compared to healthy subjects ($P < 0.05$).

Conclusions

Retinal and choriocapillaris vascular nonperfusion in OCTA is correlated significantly with disease severity in eyes with DR. Higher flow in the SCP may be an early marker of diabetic microvascular changes before clinical signs of DR. The steep decline of blood flow in the DCP with increasing DR severity suggests that alterations at the DCP warrant further investigation.

Discriminatory Power of Superficial Vessel Density and Prelaminar Vascular Flow Index in Eyes with Glaucoma and Ocular Hypertension and Normal Eyes.

Chihara E¹, Dimitrova G², Amano H¹, Chihara T³.

Purpose

We evaluate the ability of optical coherence tomography angiography parameters, such as the peripapillary vessel density of the superficial retina and prelaminar flow index of the optic disc (PLFI), to differentiate primary open-angle glaucoma (POAG) and ocular hypertension (OH) from normal eyes.

Methods

The vessel density, PLFI, mean deviation of the visual field, circumpapillary retinal nerve fiber layer thickness (cpNFLT), and global loss volume of the ganglion cell complex were evaluated in one eye of 105 subjects with POAG and OH and normal eyes. The discriminatory powers of these parameters were evaluated based on the area under the curve (AUC) of the receiver operation characteristic curve and multiple comparisons.

Results

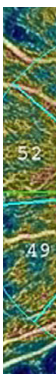
The vessel density ($P < 0.001$) and PLFI/unit area (PLFI/UA; $P = 0.020$) in eyes with POAG were significantly less than in normal eyes. The vessel density in eyes with OH was significantly ($P = 0.018$) reduced, whereas the PLFI/UA, global loss volume and cpNFLT were unaffected. The AUCs of the vessel density to discriminate glaucoma and OH from normal eyes were 0.832 and 0.724, respectively, and were significantly better than the PLFI/UA, in which the AUCs were 0.662 ($P = 0.002$) and 0.569 ($P = 0.038$), respectively. The powers of the vessel density and PLFI/UA to discriminate POAG from normal eyes were inferior to the global loss volume ($P = 0.006$ and <0.0001) and cpNFLT ($P = 0.055$ and $P < 0.0001$, respectively).

Conclusions

The vessel density and PLFI/UA decreased significantly in glaucomatous eyes. The vessel density was more efficient than the PLFI/UA for differentiating glaucoma and OH from normal eyes.



ABSTRACTS



Quantitative OCT Angiography of the Retinal Microvasculature and the Choriocapillaris in Myopic Eyes.

Al-Sheikh M¹, Phasukkijwatana N², Dolz-Marco R³, Rahimi M⁴, Iafe NA⁵, Freund KB⁶, Sadda SR⁷, Sarraf D⁸.

Purpose

To study the retinal capillary microvasculature and the choriocapillaris (CC) in myopic eyes using quantitative optical coherence tomography angiography (OCTA) analysis.

Methods

Macular OCTA images of 3 × 3 mm were obtained using the RTVue-XR Avanti with AngioVue (Fremont, CA, USA). Quantitative measurements of the retinal capillary microvascular layers and the CC were analyzed using en face projection images. Vessel density and fractal dimension of the superficial and deep retinal capillary plexus, and area and density of flow reduction in the CC were analyzed, quantified, and compared with an age-matched control group.

Results

Fifty eyes with myopia and 34 age-matched healthy eyes were included in this study. The vessel density and the vessel branching complexity using fractal dimension of the retinal capillary microvasculature were significantly lower in myopic eyes ($P < 0.001$ and $P = 0.001$). The total number of flow voids in the CC was lower (108.93 vs. 138.63, $P = 0.001$) but the total and average flow void area was significantly higher (total area 3.715 ± 0.257 vs. 3.596 ± 0.194 mm², $P = 0.026$; average area 0.044 ± 0.029 vs. 0.028 ± 0.010 mm², $P = 0.002$) compared with the healthy control group. Average choroidal thickness was lower in the myopic group versus the normal control cohort (123.538 ± 73.477 vs. 246.97 ± 41.745 μ m, $P < 0.05$) and significantly reduced in eyes with lacquer cracks (LC) compared with myopic eyes without LC formation ($P = 0.003$). There was no correlation between choroidal thickness and quantitative parameters of the CC in the myopic eyes.

Conclusions

The density of the retinal capillary microvasculature is reduced and the area of flow deficit in the CC is increased in eyes with greater myopia. The relevance of microvascular alterations in the setting of myopia warrants further study.

Retinal Vessel Density in Optical Coherence Tomography Angiography in Optic Atrophy after Nonarteritic Anterior Ischemic Optic Neuropathy.

Liu CH¹, Kao LY¹, Sun MH¹, Wu WC¹, Chen HS¹.

Aims

To compare optical coherence tomography angiography (OCTA) retinal vasculature measurements between normal and optic atrophy after nonarteritic anterior ischemic optic neuropathy (NAION) subjects.

Design

This prospective observational study was conducted between July 2015 and August 2016 at the ophthalmology outpatient department of a referral center in Taiwan. Peripapillary (4.5×4.5 mm) and parafoveal (6×6 mm) OCTA scans were acquired. Measurements of the peripapillary region were obtained in two areas: (1) circumpapillary vessel density (cpVD) and (2) whole enface image vessel density (wiVD).

Results

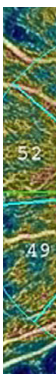
13 participants with optic atrophy after NAION had lower peripapillary vessel density than the 18 age-matched participants in the healthy control (HC) group ($p < 0.001$ for both cpVD and wiVD). However, the parafoveal vessel density was not significantly different between the two groups ($p = 0.49$). The areas under the receiver operating characteristic curve for the HC and NAION eyes were 0.992 for cpVD and 0.970 for wiVD. cpVD and wiVD were significantly correlated with the average retinal nerve fiber layer thickness ($p < 0.001$ for both).

Conclusion

Peripapillary retinal perfusion is significantly decreased in optic atrophy after NAION. OCTA may aid in the understanding of structure-function-perfusion relationships in NAION.



ABSTRACTS



Quantitative Retinal Optical Coherence Tomography Angiography in Patients with Diabetes without Diabetic Retinopathy.

Dimitrova G¹, Chihara E², Takahashi H², Amano H², Okazaki K².

Purpose

To compare optical coherence tomography (OCT) angiographic parameters in retina and choriocapillaris between control subjects and diabetic patients without diabetic retinopathy (NDR). Correlations were studied between OCT angiography parameters, retinal structure parameters, and systemic characteristics in all subjects.

Methods

Sixty-two patients were included in the study: control subjects (n = 33) and patients with NDR (n = 29). Optical coherence tomography angiographic parameters were as follows: vessel density (%) (in superficial, deep retinal vessel plexus and in choriocapillary layer) and foveal avascular zone (FAZ) area (mm²) in superficial and deep retinal vessel plexus of parafovea. Split-spectrum amplitude decorrelation angiography (SSADA) software algorithm was used for evaluation of vessel density and FAZ area (nonflow area tool). Spectral-domain OCT was used to assess full, inner, and outer retinal thickness and volume in parafovea.

Results

In superficial and deep retina, vessel densities in NDR ($44.35\% \pm 13.31\%$ and $31.03\% \pm 16.33\%$) were decreased as compared to control subjects ($51.39\% \pm 13.05\%$, $P = 0.04$; and $41.53\% \pm 14.08\%$, $P < 0.01$). Foveal avascular zone in superficial retina of NDR patients (0.37 ± 0.11 mm²) was greater than in controls (0.31 ± 0.10 mm², $P = 0.02$). Superficial vessel density significantly correlated with full retinal thickness and volume in parafovea ($r = 0.43$, $P = 0.01$; $r = 0.43$, $P = 0.01$) and with outer retinal volume in parafovea ($r = 0.35$, $P < 0.05$) of healthy subjects. Systolic blood pressure and ocular perfusion pressure significantly correlated with deep vessel density in NDR ($r = -0.45$, $P = 0.02$; $r = -0.46$, $P = 0.01$), but not in controls.

Conclusions

Superficial and deep retinal vessel density in parafovea of diabetic patients without diabetic retinopathy are both decreased compared to healthy subjects. The associations between vessel density with retinal tissue thickness and with subject's clinical characteristics differ between healthy subjects and patients with NDR.

Reduced Retinal Vessel Density in Obstructive Sleep Apnea Syndrome Patients: An Optical Coherence Tomography Angiography Study.

Yu J¹, Xiao K², Huang J², Sun X¹, Jiang C³.

Purpose

To examine the retinal vasculature in patients with obstructive sleep apnea-hypopnea syndrome (OSAS) and to determine the correlation between retinal vascularity and the severity of OSAS.

Design

Prospective, cross-sectional study.

Methods

Sixty-nine consecutive subjects who underwent polysomnography were enrolled. Patients were divided into three groups according to the severity of OSAS, which was defined using the apnea-hypopnea index (AHI) as normal-to-mild (AHI <15), moderate (≥ 15 to <30), or severe (≥ 30). The vessel densities, and macular and retinal nerve fiber layer thicknesses were compared among the three groups. The correlations between clinical variables (age, heart rate, body mass index, ocular perfusion pressure, spherical equivalence, IOP, inner retinal thickness, and AHI) and vessel densities were also determined.

Results

The full and inner parafoveal retinal thickness and the retinal nerve fiber layer thickness were similar in all three groups. The retinal vessel density decreased with greater severity of OSAS. The decrease in vessel density differed between the peripapillary and parafoveal areas. The moderate group had a significantly lower vessel density than the normal-to-mild group in the peripapillary area ($P < 0.05$), but similar vessel density as the normal-to-mild group in the parafoveal area ($P > 0.05$). The vessel densities in the parafoveal and peripapillary areas were significantly and negatively correlated with AHI (both $P < 0.05$); the relative reduction in vessel density was greater in the peripapillary area than in the parafoveal area.

Conclusions

In OSAS patients, the vessel densities in the peripapillary and parafoveal areas decreased with greater disease severity, and the decrease was more prominent in the peripapillary area.



Progressive Macula Vessel Density Loss in Primary Open-Angle Glaucoma: A Longitudinal Study.

Shoji T¹, Zangwill LM², Akagi T³, Saunders LJ², Yarmohammadi A², Manalastas PIC², Penteadó RC², Weinreb RN⁴.

Purpose

To characterize the rate of macula vessel density loss in primary open-angle glaucoma (POAG), glaucoma-suspect, and healthy eyes.

Design

Longitudinal, observational cohort from the Diagnostic Innovations in Glaucoma Study.

Methods

One hundred eyes (32 POAG, 30 glaucoma-suspect, and 38 healthy) followed for at least 1 year with optical coherence tomography angiography (OCTA) imaging on at least 2 visits were included. Vessel density was calculated in the macula superficial layer. The rate of change was compared across diagnostic groups using a multivariate linear mixed-effects model.

Results

Baseline macula vessel density was highest in healthy eyes, followed by glaucoma-suspect and POAG eyes ($P < .01$). The rate of vessel density loss was significantly different from zero in the POAG, but not in the glaucoma-suspect or healthy eyes. The mean rate of change in macula whole en face vessel density was significantly faster in glaucoma eyes ($-2.23\%/y$) than in glaucoma-suspect ($0.87\%/y$, $P = .001$) or healthy eyes ($0.29\%/y$, $P = .004$). Conversely, the rate of change in ganglion cell complex (GCC) thickness was not significantly different from zero in any diagnostic group, and no significant differences in the rate of GCC change among diagnostic groups were found.

Conclusions

With a mean follow-up of less than 14 months, eyes with POAG had significantly faster loss of macula vessel density than either glaucoma-suspect or healthy eyes. Serial OCTA measurements also detected glaucomatous change in macula vessel density in eyes without evidence of change in GCC thickness.

Optical Coherence Tomography Angiography Vessel Density in Children with Type 1 Diabetes.

Gołębiewska J¹, Olechowski A¹, Wysocka-Mincewicz M², Odrobina D^{3,4}, Baszyńska-Wilk M², Groszek A², Szalecki M^{2,3}, Hautz W¹.

Purpose

To assess the optical coherence tomography angiography (OCTA) retinal vessel density and foveal avascular zone (FAZ) in children with type 1 diabetes (T1D) and compare potential pathologic early changes in this population to healthy age-matched controls.

Methods

This study included 130 pubescent children: 94 with T1D (188 eyes) and 36 of their age-matched control group (60 eyes). OCTA was performed using AngioVue (Avanti, Optovue, Fremont, CA, USA). FAZ area (mm²) in superficial plexus, whole superficial capillary vessel density (wsVD), fovea superficial vessel density (fsVD), parafovea superficial vessel density (psVD), whole deep vessel density (wdVD), fovea deep vessel density (fdVD), parafovea deep vessel density (pdVD), foveal thickness (FT) (μm) and parafoveal thickness (PFT) (μm) were taken into analysis. Among the studied patients with T1D there were assessed codependences regarding the investigated foveal and parafoveal parameters and selected potential predictors, i.e. patient's age (years), diabetes duration time (years), age of onset of the disease (years), mean level of glycosylated hemoglobin (HbA1C) (%), and concentration of serum creatinine (mg/dL).

Results

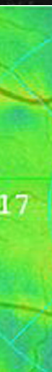
None of the abovementioned OCT and OCTA parameters was statistically significantly different between the groups. The patient's age statistically significantly did not influence any of the OCT and OCTA parameters. Yet an elevated level of HbA1C tended to reduce the parafovea superficial vessel density ($p = 0.039$), and parafoveal thickness ($p = 0.003$) and an increased serum creatinine level correlated with the decreased whole deep vessel density ($p < 0.001$). The parafovea deep vessel density in the diabetic patients decreased when the serum creatinine level ($p = 0.008$), age of onset of the disease ($p = 0.028$), and diabetes duration time ($p = 0.014$) rose.

Conclusions

Vessel density, both in superficial and deep plexuses, and FAZ area are normal in pubescent children with T1D comparing to healthy subjects. An elevated level of HbA1C correlated with reduced psVD and PFT. Longitudinal observation of these young patients is needed to determine if any of these OCTA measurements are predictive of future DR severity.



ABSTRACTS



Optical Coherence Tomography Angiography in Retinal Vein Occlusion: Correlations between Macular Vascular Density, Visual Acuity, and Peripheral Nonperfusion Area on Fluorescein Angiography.

Seknazi D¹, Coscas F, Sellam A, Rouimi F, Coscas G, Souied EH, Glacet-Bernard A.

Purpose

To study correlations in patients with retinal vein occlusion between the automatically quantified macular vascular densities in the superficial and deep capillary plexus (DCP) obtained using optical coherence tomography angiography (OCTA) and the data from conventional examination, particularly visual acuity and peripheral retinal nonperfusion assessed using fluorescein angiography (FA).

Methods

Retrospective, observational study of patients with retinal vein occlusion who underwent a comprehensive ophthalmic examination including FA and OCTA using the AngioVue OCTA system version 2015.100.0.35 (RTVue XR; Avanti; Optovue, Inc. Fremont, CA, USA). Vascular densities in the superficial capillary plexus and DCP, as well as the area of the foveal avascular zone, were measured using the AngioAnalytics™ software.

Results

Our study of 65 eyes of 61 patients (33 men, mean age: 67 years) showed a significant correlation between peripheral nonperfusion on FA and (1) automatically quantified global vascular density in both plexus ($P = 0.021$ for the DCP) and (2) foveal avascular zone area ($P = 0.037$). We also found significant correlations between capillary dropouts in both plexus and peripheral nonperfusion ($P < 0.001$ for both) and between visual acuity and vascular densities ($P = 0.002$ for the global density in the DCP). Global density less than 46% in the DCP was associated to the presence of peripheral nonperfusion area on FA ($P = 0.003$) and to enlargement of the superficial foveal avascular zone ($P = 0.002$).

Conclusion

Our study demonstrated a significant correlation between automatically quantified macular vascular density on OCTA and peripheral nonperfusion on FA; OCTA could help identify high-risk retinal vein occlusion patients who may benefit from further evaluation using FA. This is an open-access article distributed under the terms of the Creative Commons Attribution-Non Commercial-No Derivatives License 4.0 (CCBY-NC-ND), where it is permissible to download and share the work provided it is properly cited. The work cannot be changed in any way or used commercially without permission from the journal.

OCTA Bibliography: Peer-Reviewed Articles

Highlighting AngioAnalytics™

2017

1. Aggarwal K, Agarwal A, Deokar A, Mahajan S, Singh R, Bansal R, Sharma A, Dogra MR, Gupta V; OCTA Study Group. Distinguishing Features of Acute Vogt-Koyanagi-Harada Disease and Acute Central Serous Chorioretinopathy on Optical Coherence Tomography Angiography and En Face Optical Coherence Tomography Imaging. *J Ophthalmic Inflamm Infect*. 2017 Dec;7(1):3. Epub 2017 Jan 13.
2. Alten F, Lauermaun JL, Clemens CR, Heiduschka P, Eter N. Signal Reduction in Choriocapillaris and Segmentation Errors in Spectral Domain OCT Angiography Caused by Soft Drusen. *Graefes Arch Clin Exp Ophthalmol*. 2017 Oct 5. [Epub ahead of print].
3. Al-Sheikh M1, Phasukkijwatana N2, Dalz-Marco R3, Rahimi M4, Iafe NA5, Freund KB6, Sadda SR7, Sarraf D8. Quantitative OCT Angiography of the Retinal Microvasculature and the Choriocapillaris in Myopic Eyes. *Invest Ophthalmol Vis Sci*. 2017.
4. Amoroso F1,2, Miere A1, Semoun O1, Jung C1,3, Capuano V1, Souied EH1,3. Optical Coherence Tomography Angiography Reproducibility of Lesion Size Measurements in Neovascular Age-Related Macular Degeneration (AMD). *Br J Ophthalmol*. 2017.
5. Azevedo AGB, Lima LH, Müller L, Filho FR, Zett C, Maia A, Roisman L. Anatomical and Functional Correlation in Susac Syndrome: Multimodal Imaging Assessment. *Int J Retina Vitreous*. 2017 Oct 16;3:39.
6. Bazzazi N, Akbarzadeh S, Yavarikia M, Poorolajal J, Fouladi DF. High Myopia and Diabetic Retinopathy: A Contralateral Eye Study in Diabetic Patients with High Myopic Anisometropia. *Retina*. 2017 Jul;37(7):1270-1276.
7. Borrelli E, Uji A, Sarraf D, Sadda SR. Alterations in the Choriocapillaris in Intermediate Age-Related Macular Degeneration. *Invest Ophthalmol Vis Sci*. 2017 Sep;58:4792-4798.
8. Brand C, Zitzmann M, Eter N, Kliesch S, Wistuba J, Alnawaiseh M, Heiduschka P. Aberrant Ocular Architecture and Function in Patients with Klinefelter Syndrome. *Sci Rep*. 2017 Oct 13;7(1):13130.
9. Chang MY, Phasukkijwatana N, Garrity S, Pineles SL, Rahimi M, Sarraf D, Johnston M, Charles A, Arnold AC. Foveal and Peripapillary Vascular Decrement in Migraine with Aura Demonstrated by Optical Coherence Tomography Angiography. *Invest Ophthalmol Vis Sci*. 2017 Oct 1;58(12):5477-5484.
10. Chen Q, Ma Q, Wu C, Tan F, Chen F, Wu Q, Zhou R, Zhuang X, Lu F, Qu J, Shen M. Macular Vascular Fractal Dimension in the Deep Capillary Layer as an Early Indicator of Microvascular Loss for Retinopathy in Type 2 Diabetic Patients. *Invest Ophthalmol Vis Sci*. 2017 Jul 1;58(9):3785-3794.
11. Chi YT, Yang CH, Cheng CK. Optical Coherence Tomography Angiography for Assessment of the 3-Dimensional Structures of Polypoidal Choroidal Vasculopathy. *JAMA Ophthalmol*. 2017 Oct 19. [Epub ahead of print].
12. Chiara M, Eandi; Antonio Ciardella; Mariacristina Parravano; Filippo Missiroli; Camilla Alovisi; Chiara Veronese; Maria C. Morara; Massimo Grossi; Gianni Virgili; Federico Ricci. Indocyanine Green Angiography and Optical Coherence Tomography Angiography of Choroidal Neovascularization in Age-Related Macular Degeneration. *Invest Ophthalmol Vis Sci*. 2017.
13. Chihara E1, Dimitrova G2, Amano H1, Chihara T3. Discriminatory Power of Superficial Vessel Density and Prelaminar Vascular Flow Index in Eyes with Glaucoma and Ocular Hypertension and Normal Eyes. *Invest Ophthalmol Vis Sci*. 2017.
14. Dehghani C, Srinivasan S, Edwards K, Pritchard N, Russell AW, Malik RA, Efron N. Presence of Peripheral Neuropathy Is Associated with Progressive Thinning of Retinal Nerve Fiber Layer in Type 1 Diabetes. *Invest Ophthalmol Vis Sci*. 2017 May 1;58(6):BIO234-BIO239.
15. Dimitrova G1, Chihara E2, Takahashi H2, Amano H2, Okazaki K2. Quantitative Retinal Optical Coherence Tomography Angiography in Patients with Diabetes without Diabetic Retinopathy. *Invest Ophthalmol Vis Sci*. 2017.
16. Faridi A, Jia Y, Gao SS, Huang D, Bhavsar KV, Wilson DJ, Sill A, Flaxel CJ, Hwang TS, Lauer AK, Bailey ST. Sensitivity and Specificity of OCT Angiography to Detect Choroidal Neovascularization. *Ophthalmol Retina*. 2017 Jul-Aug;1(4):294-303.
17. Garrity ST, Iafe NA, Phasukkijwatana N, Chen X, Sarraf D. Quantitative Analysis of Three Distinct Retinal Capillary Plexuses in Healthy Eyes Using Optical Coherence Tomography Angiography. *Invest Ophthalmol Vis Sci*. 2017 Oct 1;58(12):5548-5555.
18. Gołębiewska J, Olechowski A, Wysocka-Mincewicz M, Odrobina D, Baszyńska-Wilk M, Groszek A, Szalecki M, Hautz W. Optical Coherence Tomography Angiography Vessel Density in Children with Type 1 Diabetes. *PLoS One*. 2017 Oct 20;12(10):e0186479.
19. Ichiyama Y, Sawada T, Ito Y, Kakinoki M, Ohji M. Optical Coherence Tomography Angiography Reveals Blood Flow in Choroidal Neovascular Membrane in Remission Phase of Neovascular Age-Related Macular Degeneration. *Retina*. 2017 Apr;37(4):724-730.
20. Jacobson SG, Cideciyan AV, Sumaroka A, Roman AJ, Charrng J, Lu M, Choi W, Sheplock R, Swider M, Kosyk MS, Schwartz SB, Stone EM, Fishman GA. Outcome Measures for Clinical Trials of Leber Congenital Amaurosis Caused by the Intronic Mutation in the CEP290 Gene. *Invest Ophthalmol Vis Sci*. 2017 May 1;58(5):2609-2622.
21. Jia SS, Zhao C, Gong D, Chen Z, Zhang MF. [Optical Coherence Tomography Angiography of Acute Vogt-Koyanagi-Harada disease]. [Article in Chinese; Abstract available in Chinese from the publisher]. *Zhonghua Yan Ke Za Zhi*. 2017 Oct 11;53(10):735-739.
22. Jia Y, Simonett JM, Wang J, Hua X, Liu L, Hwang TS, Huang D. Wide-Field OCT Angiography Investigation of the Relationship between Radial Peripapillary Capillary Plexus Density and Nerve Fiber Layer Thickness. *Invest Ophthalmol Vis Sci*. 2017 Oct 1;58(12):5188-5194.
23. Kaizu Y, Nakao S, Yoshida S, Hayami T, Arima M, Yamaguchi M, Wada I, Hisatomi T, Ikeda Y, Ishibashi T, Sonoda KH. Optical Coherence Tomography Angiography Reveals Spatial Bias of Macular Capillary Dropout in Diabetic Retinopathy. *Invest Ophthalmol Vis Sci*. 2017 Sep;58:4889-4897.
24. Kang JW, Yoo R, Jo YH, Kim HC. Correlation of Microvascular Structures on Optical Coherence Tomography Angiography with Visual Acuity in Retinal Vein Occlusion. *Retina*. 2017 Sep;37(9):1700-1709.

25. Kvant A, Casselholm de Salles M, Amrén U, Bartuma H. Optical Coherence Tomography Angiography of the Foveal Microvasculature in Geographic Atrophy. *Retina*. 2017 May;37(5):936-942.
26. Liu CH1, Kao LY1, Sun MH1, Wu WC1, Chen HS1. Retinal Vessel Density in Optical Coherence Tomography Angiography in Optic Atrophy after Nonarteritic Anterior Ischemic Optic Neuropathy. *J Ophthalmol*. 2017.
27. Manabe S, Osaka R, Nakano Y, Takasago Y, Fujita T, Shiragami C, Hirooka K, Muraoka Y, Tsujikawa A. Association between Parafoveal Capillary Nonperfusion and Macular Function in Eyes with Branch Retinal Vein Occlusion. *Retina*. 2017 Sep;37(9):1731-1737.
28. Marsh-Tootle WL, Harb E, Hou W, Zhang Q, Anderson HA, Weise K, Norton TT, Gwiazda J, Hyman L; for the Correction of Myopia Evaluation Trial (COMET) Study Group. Optic Nerve Tilt, Crescent, Ovality, and Torsion in a Multi-Ethnic Cohort of Young Adults with and without Myopia. *Invest Ophthalmol Vis Sci*. 2017 Jun 1;58(7):3158-3171.
29. Mastropasqua R, Toto L, Mastropasqua A, Aloia R, De Nicola C, Mattei PA, Di Marzio G, Di Nicola M, Di Antonio L. Foveal Avascular Zone Area and Parafoveal Vessel Density Measurements in Different Stages of Diabetic Retinopathy by Optical Coherence Tomography Angiography. *Int J Ophthalmol*. 2017 Oct 18;10(10):1545-1551.
30. Nesper PL, Roberts PK, Onishi AC, Chai H, Liu L, Jampol LM, Fawzi AA. Quantifying Microvascular Abnormalities with Increasing Severity of Diabetic Retinopathy Using Optical Coherence Tomography Angiography. *Invest Ophthalmol Vis Sci*. 2017 May 1;58(6):BIO307-BIO315.
31. Rao HL, Pradhan ZS, Weinreb RN, Dasari S, Riyazuddin M, Venugopal JP, Puttaiah NK, Rao DAS, Devi S, Mansouri K, Webers CAB. Optical Coherence Tomography Angiography Vessel Density Measurements in Eyes with Primary Open-Angle Glaucoma and Disc Hemorrhage. *J Glaucoma*. 2017 Oct;26(10):888-895.
32. Roberts PK, Nesper PL, Gill MK, Fawzi AA. Semiautomated Quantitative Approach to Characterize Treatment Response in Neovascular Age-Related Macular Degeneration: A Real-World Study. *Retina*. 2017 Aug;37(8):1492-1498.
33. Sakaguchi K, Higashide T, Udagawa S, Ohkubo S, Sugiyama K. Comparison of Sectoral Structure-Function Relationships in Glaucoma: Vessel Density versus Thickness in the Peripapillary Retinal Nerve Fiber Layer. *Invest Ophthalmol Vis Sci*. 2017 Oct 1;58(12):5251-5262.
34. Say EAT, Ferenczy S, Magrath GN, Samara WA, Khoo CTL, Shields CL. Image Quality and Artifacts on Optical Coherence Tomography Angiography: Comparison of Pathologic and Paired Fellow Eyes in 65 Patients with Unilateral Choroidal Melanoma Treated with Plaque Radiotherapy. *Retina*. 2017 Sep;37(9):1660-1673.
35. Seknazi D1, Coscas F, Sellam A, Rouimi F, Coscas G, Souied EH, Glacet-Bernard A. Optical Coherence Tomography Angiography in Retinal Vein Occlusion: Correlations between Macular Vascular Density, Visual Acuity, and Peripheral Nonperfusion Area on Fluorescein Angiography. *Retina*. 2017.
36. Shoji T1, Zangwill LM2, Akagi T3, Saunders LJ2, Yarmohammadi A2, Manalastas PIC2, Penteado RC2, Weinreb RN4. Progressive Macula Vessel Density Loss in Primary Open-Angle Glaucoma: A Longitudinal Study. *Am J Ophthalmol*. 2017.
37. Song Y, Min JY, Mao L, Gong YY. Microvasculature Dropout Detected by the Optical Coherence Tomography Angiography in Nonarteritic Anterior Ischemic Optic Neuropathy. *Lasers Surg Med*. 2017 Oct 7. [Epub ahead of print].
38. Spaide RF. Microvascular Flow Abnormalities Associated with Retinal Vasculitis: A Potential of Mechanism of Retinal Injury. *Retina*. 2017 Jun;37(6):1034-1042.
39. Stopa M, Marciniak E, Rakowicz P, Stankiewicz A, Marciniak T, Dąbrowski A. Imaging and Measurement of the Preretinal Space in Vitreomacular Adhesion and Vitreomacular Traction by a New Spectral Domain Optical Coherence Tomography Analysis. *Retina*. 2017 Oct;37(10):1839-1846.
40. Tan ACS, Yzer S, Freund KB, Dansingani KK, Phasukkijwatana N, Sarraf D. Choroidal Changes Associated with Serous Macular Detachment in Eyes with Staphyloma, Dome-Shaped Macula or Tilted Disk Syndrome. *Retina*. 2017 Aug;37(8):1544-1554.
41. Toto, 1 Rossella D'Aloisio, 2, * Marta Di Nicola, 3 Giuseppe Di Martino, 4 Silvio Di Staso, 5 Marco Ciancaglini, 5 Daniele Tognetto, 2 and Leonardo Mastropasqua 1. Qualitative and Quantitative Assessment of Vascular Changes in Diabetic Macular Edema after Dexamethasone Implant Using Optical Coherence Tomography Angiography. *Int J Mol Sci*. 2017.
42. Tsuboi K, Ishida Y, Kamei M. Gap in Capillary Perfusion on Optical Coherence Tomography Angiography Associated with Persistent Macular Edema in Branch Retinal Vein Occlusion. *Invest Ophthalmol Vis Sci*. 2017 Apr 1;58(4):2038-2043.
43. Yilmaz I1, Ocak OB2, Yilmaz BS2, Inal A2, Gokyigit B2, Taskapili M2. Comparison of Quantitative Measurement of Foveal Avascular Zone and Macular Vessel Density in Eyes of Children with Amblyopia and Healthy Controls: An Optical Coherence Tomography Angiography Study. *Journal of AAPOS*. 2017.
44. Yu J, Xiao K, Huang J, Sun X, Jiang C. Reduced Retinal Vessel Density in Obstructive Sleep Apnea Syndrome Patients: An Optical Coherence Tomography Angiography Study. *Invest Ophthalmol Vis Sci*. 2017 Jul 1;58(9):3506-3512.
45. Zahid S, Chen KC, Jung JJ, Balaratnasingam C, Ghadiali Q, Sorenson J, Rofagha S, Freund KB, Yannuzzi LA. Optical Coherence Tomography Angiography of Chorioretinal Lesions Due to Idiopathic Multifocal Choroiditis. *Retina*. 2017 Aug;37(8):1451-1463.

2016 (November and December)

1. Kumar RS, Anegondi N, Chandapura RS, Sudhakaran S, Kadambi SV, Rao HL, Aung T, Sinha Roy A. Discriminant Function of Optical Coherence Tomography Angiography to Determine Disease Severity in Glaucoma. *Invest Ophthalmol Vis Sci*. 2016 Nov 1;57(14):6079-6088.
2. La Spina C, Carnevali A, Marchese A, Querques G, Bandello F. Reproducibility and Reliability of Optical Coherence Tomography Angiography for Foveal Avascular Zone Evaluation and Measurement in Different Settings. *Retina*. 2016 Dec 20. [Epub ahead of print].
3. Lee EJ, Lee KM, Lee SH, Kim TW. OCT Angiography of the Peripapillary Retina in Primary Open-Angle Glaucoma. *Invest Ophthalmol Vis Sci*. 2016 Nov 1;57(14):6265-6270.
4. Lee J, Rosen R. Optical Coherence Tomography Angiography in Diabetes. *Curr Diab Rep*. 2016 Dec;16(12):123.
5. Li M, Wang H, Liu Y, Zhang X, Wang N. Comparison of Time-Domain, Spectral-Domain and Swept-Source OCT in Evaluating Aqueous Cells In Vitro. *Sci China Life Sci*. 2016 Dec;59(12):1319-1323. Epub 2016 Nov 4.



6. Liang MC, de Carlo TE, Baurnal CR, Reichel E, Waheed NK, Duker JS, Witkin AJ. Correlation of Spectral Domain Optical Coherence Tomography Angiography and Clinical Activity in Neovascular Age-Related Macular Degeneration. *Retina*. 2016 Dec;36(12):2265-2273.
7. Magrath GN, Say EA, Sioufi K, Ferenczy S, Samara WA, Shields CL. Variability in Foveal Avascular Zone and Capillary Density Using Optical Coherence Tomography Angiography Machines in Healthy Eyes. *Retina*. 2016 Dec 16. [Epub ahead of print].
8. Mandadi SK, Agarwal A, Aggarwal K, Moharana B, Singh R, Sharma A, Bansal R, Dogra MR, Gupta V; for OCTA Study Group. Novel Findings on Optical Coherence Tomography Angiography in Patients with Tubercular Serpiginous-Like Choroiditis. *Retina*. 2017 Sep;37(9):1647-1659. Epub 2016 Dec 7.
9. Mané V, Dupas B, Gaudric A, Bonnin S, Pedinielli A, Bousquet E, Erginay A, Tadayoni R, Couturier A. Correlation between Cystoid Spaces in Chronic Diabetic Macular Edema and Capillary Nonperfusion Detected by Optical Coherence Tomography Angiography. *Retina*. 2016 Dec;36 Suppl 1:S102-S110.
10. Mansoori T, Sivaswamy J, Gamalapati JS, Agraharam SG, Balakrishna N. Measurement of Radial Peripapillary Capillary Density in the Normal Human Retina Using Optical Coherence Tomography Angiography. *J Glaucoma*. 2016 Nov 30. [Epub ahead of print].
11. Maruko I, Koizumi H, Hasegawa T, Iida T. Detection of Retrobulbar Blood Vessels in Optical Coherence Tomography Angiographic Images in Eyes with Pathologic Myopia. *Am J Ophthalmol Case Reports*. 2016 Dec;4:74-77. Epub 2016 Oct 4.
12. Mo J, Duan AL, Chan SY, Wang XF, Wei WB. Application of Optical Coherence Tomography Angiography in Assessment of Posterior Scleral Reinforcement for Pathologic Myopia. *Int J Ophthalmol*. 2016 Dec 18;9(12):1761-1765.
13. Pakzad-Vaezi K, Keane PA, Cardoso JN, Egan C, Tufail A. Optical Coherence Tomography Angiography of Foveal Hypoplasia. *Br J Ophthalmol*. 2017 Jul;101(7):985-988. Epub 2016 Nov 29.
14. Patel RC, Gao SS, Zhang M, Alabduljalil T, Al-Qahtani A, Weleber RG, Yang P, Jia Y, Huang D, Pennesi ME. Optical Coherence Tomography Angiography of Choroidal Neovascularization in Four Inherited Retinal Dystrophies. *Retina*. 2016 Dec;36(12):2339-2347.
15. Pichi F, Srivastava SK, Chexal S, Lembo A, Lima LH, Neri P, Saitta A, Chhablani J, Albini TA, Nucci P, Freund KB, Chung H, Lowder CY, Sarraf D. En Face Optical Coherence Tomography and Optical Coherence Tomography Angiography of Multiple Evanescent White Dot Syndrome: New Insights Into Pathogenesis. *Retina*. 2016 Dec;36 Suppl 1:S178-S188.
16. Rao HL, Kadambi SV, Weinreb RN, Puttaiah NK, Pradhan ZS, Rao DA, Kumar RS, Webers CA, Shetty R. Diagnostic Ability of Peripapillary Vessel Density Measurements of Optical Coherence Tomography Angiography in Primary Open-Angle and Angle-Closure Glaucoma. *Br J Ophthalmol*. 2017 Aug;101(8):1066-1070. Epub 2016 Nov 29.
17. Samara WA, Shahlaee A, Adam MK, Khan MA, Chiang A, Maguire JJ, Hsu J, Ho AC. Quantification of Diabetic Macular Ischemia Using Optical Coherence Tomography Angiography and Its Relationship with Visual Acuity. *Ophthalmology*. 2017 Feb;124(2):235-244. Epub 2016 Nov 23.
18. Skalet AH, Li Y, Lu CD, Jia Y, Lee BK, Husvagt L, Maier A, Fujimoto JG, Thomas CR, Huang D. Optical Coherence Tomography Angiography Characteristics of Iris Melanocytic Tumors. *Ophthalmology*. 2016;124(2):197-204. Epub 2016 Nov 14.
19. Tanaka K, Mori R, Kawamura A, Nakashizuka H, Wakatsuki Y, Yuzawa M. Comparison of OCT Angiography and Indocyanine Green Angiographic Findings with Subtypes of Polypoidal Choroidal Vasculopathy. *Br J Ophthalmol*. 2017 Jan;101(1):51-55. Epub 2016 Dec 2.
20. Toto L, Borrelli E, Mastropasqua R, Senatore A, Di Antonio L, Di Nicola M, Carpineto P, Mastropasqua L. Macular Features in Retinitis Pigmentosa: Correlations among Ganglion Cell Complex Thickness, Capillary Density, and Macular Function. *Invest Ophthalmol Vis Sci*. 2016 Nov 1;57(14):6360-6366.
21. Yang Y, Wang J, Jiang H, Yang X, Feng L, Hu L, Wang L, Lu F, Shen M. Retinal Microvasculature Alteration in High Myopia. *Invest Ophthalmol Vis Sci*. 2016 Nov 1;57(14):6020-6030.
22. You Q, Freeman WR, Weinreb RN, Zangwill L, Manalastas PI, Saunders IJ, Nudleman E. Reproducibility of Vessel Density Measurement with Optical Coherence Tomography Angiography in Eyes with and without Retinopathy. *Retina*. 2017 Aug;37(8):1475-1482. Epub 2016 Dec 7.



Our vision is foresight

2800 Bayview Drive, Fremont, CA 94538 +1.510.623.8868 optovue.com

©2017 Optovue, Inc. Optovue, AngioVue, AngioAnalytics and DualTrac are trademarks or registered trademarks of Optovue, Inc. All rights reserved.

